Green Chemistry

One-Step Lignocellulose Depolymerization and Saccharification to High Sugar Yield and Less Condensed Isolated Lignin

Journal:	*Green Chemistry*
Manuscript ID	GC-ART-12-2020-004119
Article Type:	Paper
Date Submitted by the Author:	05-Dec-2020
Complete List of Authors:	Sadula, Sunitha; University of Delaware, Catalysis Center for Energy Innovation Rodriguez Quiroz, Natalia; University of Delaware, Chemical Engineering; Catalysis Center for Energy Innovation, Athaley, Abhay ; University of Delaware, Catalysis Center for Energy Innovation Ebikade, Osamudiamhen; University of Delaware, Chemical and Biomolecular Engineering; University of Delaware, Chemical and Biomolecular Engineering Ierapetritou, Marianthi; University of Delaware, Vlachos, Dion; Univ. of Delaware, Chemical Engineering Saha, Basudeb; University of Delaware, Catalysis Center for Energy Innovation;

One-Step Lignocellulose Depolymerization and Saccharification to High Sugar Yield and Less Condensed Isolated Lignin

Sunitha Sadula,[1] Natalia Rodriguez Quiroz,[1,2] Abhay Athaley,[1,2] Elvis Osamudiamhen Ebikade,[1,2] Marianthi Ierapetritou,[1,2] Dionisios G. Vlachos,*[1,2] and Basudeb Saha*[1]

[1]Catalysis Center for Energy Innovation, 221 Academy St., University of Delaware, Newark, Delaware 19716, USA

[2]Department of Chemical and Biochemical Engineering, 150 Academy St., University of Delaware, Newark, Delaware 19716, USA

Abstract

The cost of sugar production remains a key challenge in future lignocellulosic biorefineries. We demonstrate that $ZnBr_2$, an inexpensive inorganic salt, provides nearly theoretical yields of glucose and xylose in one-step from poplar wood at 85 °C and short reaction times at molten salt hydrate (MSH) conditions without an acid. Catalytic depolymerization of the isolated MSH lignin, using a CoS_2 catalyst, yields 17% phenol-like monomers compared to only 1% produced from the acidified MSH lignin. Reductive catalytic fraction of MSH lignin over Ru/C resulted in two times higher total monomer yield compared to the AMSH lignin. Both the lignin samples were characterized using 2D HSQC NMR and the thioacidolysis method. Thioacidolysis studies reveal 8.4% and 1.8% of β-O-4 linkages in MSH and acidified MSH lignin, respectively. Thermodynamic modeling and ^{13}C NMR spectroscopy indicate that the effectiveness of this catalyst arises from the strong interaction of the Lewis acidic zinc cation (Zn^{2+}) with the coordinated water molecules resulting in hydrolysis of the metal aquo complex and to the salt-driven increase in the H^+ activity coefficient. Techno-economic analysis demonstrates that despite being slower, the $ZnBr_2$ MSH media has cost advantages, compared to conventional hydrolysis and even to the LiBr and $ZnBr_2$ AMSH, due to the higher quality of lignin.

Keywords: lignocellulose, biomass, hydrolysis, saccharification, depolymerization, molten salt hydrate, lignin valorization, phenols, $ZnBr_2$

Introduction

Lignocellulosic biomass, including forest wood, municipal solid waste, energy crops, and agriculture residue, is a carbon-neutral, non-edible feedstock that can supply a significant fraction of organic chemicals and biofuels in the U.S.[1-5] and mitigate global climate challenges. While efforts to commercialize several bioproducts are underway,[6] the complex carbohydrate-lignin interactions in the cell microfibril make lignocellulose recalcitrant to breakdown. Thus, pretreatment is often employed to deconstruct lignocellulose followed by conversion of the polysaccharides into soluble sugars.[7-8] This two-step process is expensive. In addition, pretreatment increases C−C linkages in lignin and make lignin depolymerization more difficult. As a result, lignin is a stream of low (e.g., heating) value.[9-11] The valorization of lignin is essential for the profitability and sustainability of future biorefineries.[12] Developing technologies that overcome these challenges is desirable.

Recent reports by our group[13-14] and other researchers show that molten salt hydrates (MSHs) can convert crystalline cellulose and lignocellulose into soluble sugars with high yield[15-20] without pretreatment. MSHs are similar to ionic liquids but are significantly cheaper. A MSH has a water to salt molar ratio close to the coordination number of the strongest hydrated cation. Acidified molten salt hydrates (AMSH), which contain a small fraction of an inorganic acid, are especially effective. In particular, LiBr-AMSH, consisting of 58 wt% LiBr and 0.05 M aqueous H_2SO_4, depolymerizes and saccharifies various untreated lignocellulosic feedstocks at 85 °C with >90% yield of soluble sugar within 1 h of reaction time.[13] While techno-economic analysis suggested favorable process economics compared to dilute and concentrated acid hydrolysis processes,[13-14] the cost of LiBr is still a drawback. In addition, the derived lignin is similar to technical lignin containing only a few C−O linkages.

Herein we report that $ZnBr_2$ MSH, without any added acid, is as effective as the LiBr AMSH in the one-step depolymerization and saccharification of raw poplar wood into high yield sugars at 85 °C. Thermodynamic modeling and ^{13}C NMR spectroscopy are used to compare the acidity of $ZnBr_2$ AMSH and $ZnBr_2$ MSH and understand the effectiveness of $ZnBr_2$ MSH. The effect of absence of acid on the lignin structure and its depolymerization into phenols is demonstrated. Techno-economic analysis (TEA) is also conducted and compared to those of LiBr AMSH and conventional hydrolysis processes.

Experimental Methods and Modeling

Materials. Zinc bromide, 5 M sulfuric acid, and HPLC standards (xylose, glucose, levoglucosan, acetic acid, formic acid, levulinic acid, 5-hydroxymethylfurfural, and furfural) were purchased from Sigma-Aldrich. Gluco- and xylo-oligosaccharides with degree of polymerization (DP) of 2-6 of >95% purity were purchased from Megazymes. Deionized water (Millipore model Direct-Q3 UV R) was used for the preparation of all solutions unless otherwise mentioned. Nylon syringe filter discs (Fisher Scientific) with 0.2 μm pore size were used for filtration of solutions for HPLC analysis. Poplar wood biomass of ~1 mm particle size was purchased from Forest Concepts, LLC. Compositional analysis of poplar wood, performed following the NREL (National Renewable Energy Laboratory) procedure,[21] shows 45.3 wt% glucan, 18 wt% xylan, 25.5 wt% lignin, 0.8 wt% ash and 5 wt% extractives (on the basis of dry weight of biomass).

Soxhlet-extracted poplar wood (SEPW) preparation. Extractives were obtained using ethanol followed by water, each for 8 h, using a soxhlet extraction apparatus. The washed sample was dried at 30 °C overnight and its moisture content was measured using a moisture analyzer (Sartorius MA160).

Saccharification. One-step depolymerization and saccharification of soxhlet extracted poplar wood was conducted in high pressure glass vials (VWR International, LLC.). First, a $ZnBr_2$ MSH solution was prepared by mixing $ZnBr_2$ (7.04 g) and pure water (2.25 mL) in a vial to give a molar ratio of water to $ZnBr_2$ of 4. For an AMSH solution, the same amount of $ZnBr_2$ was added in 0.05 M aqueous sulfuric acid (2.25 mL). Next, 0.33 g soxhlet extracted poplar wood (based on dry weight) were added into the vial containing MSH or AMSH, and the mixture was vortexed for 30 sec. Subsequently, the vial was sealed with an Al-crimp cap (CG-4920-10, Chemglass life sciences), placed in a preheated (85 °C) heating block and stirred continuously to start depolymerization and saccharification. Upon reaction for a set time, the vial was removed from the heating block and the solution was quenched in an ice bath. The hydrolysate was diluted 10 times in DI water and filtered using syringe filters for HPLC analysis. The recovered lignin was washed, dried at 105 °C for 8 h, and used for characterization and depolymerization.

Analysis of soluble products. A Waters HPLC instrument (model e2695) equipped with a photodiode array (PDA) detector (Waters 2998) and a refractive index (RI) detector (Waters 2414) was used for analysis of soluble products in the hydrolysates. Two types of HPLC

columns were used: (1) A Bio-rad Aminex HPX-87H (7.8 X 300 mm, 9 µm) column, operating at a column oven temperature of 55 °C using 0.05 M H_2SO_4 as a mobile phase at a flow rate of 0.6 mL/min, for detection and quantification of glucose (9.52 min), xylose (10.14 min), levoglucosan (12.47 min), formic acid (14.23 min), acetic acid (15.48 min), levulinic acid (16.16 min) using the RI detector. The PDA detector (254 nm) was used for analysis of 5-hydroxymethylfurfural (HMF, 30.22 min) and furfural (45.58 min). (2) An Agilent Hiplex Na (7.7 × 300 mm, 10 µm) column, operating at a column oven temperature of 85 °C using milli-Q water as the mobile phase at a flow rate of 0.2 mL/min, for analysis of gluco- and xylo-oligosaccharides of DP up to 5 using the RI detector. All products were identified on the basis of their retention times reported in our earlier publication.[13] The concentrations of each product were calculated from their respective pre-calibrated plots of peak area versus concentrations for standard samples. The yields of soluble products were calculated following our reported method.[18] The following equations were used.

C_6/C_5 monosaccharides, oligosaccharides, HMF and furfural yields were calculated on the basis of dry weight of soxhlet extracted poplar wood

$$Yield\ (wt\%) = \frac{\text{Total amount of soluble product in mg (dry weight)}}{Dry\ wt\ (mg) of\ SEPW}\ X\ 100$$

C_6/C_5 monosaccharide yields were calculated on the basis of theoretical glucan and xylan amounts in soxhlet extracted poplar wood

$$Yield\ (wt\%) = \frac{Total\ amount\ of\ soluble\ product\ in\ mg\ (dry\ weight))}{Theoretical\ glucose\ or\ xylose\ amounts\ in\ SEPW}\ X\ 100$$

Lignin characterization. Lignin from our one-step saccharification of soxhlet extracted poplar wood is referred hereto as AMSH lignin or MSH lignin and its characterization is discussed below.

Chemical composition of recovered solids. The NREL method[21] was followed to measure the amount of lignin in solids recovered during saccharification

2D HSQC NMR. 2D $^{13}C–^{1}H$ heteronuclear single quantum correlation (HSQC) NMR spectra of lignin were recorded on a Bruker AV-II spectrometer operating at 600 Hz. The sample was prepared by dissolving 50 mg of lignin in 0.75 mL d_6-DMSO. The NMR spectra were recorded at 25 °C using the standard Bruker pulse sequence hsqcetgpsi.2 and the following operating parameters: 10.3 ppm sweep width in the F2 (1H), 165 ppm sweep width F1 (13C), an

acquisition time of 130 ms, a relaxation delay time of 1.5 s, 24 scans and 1024 data points. The DMSO solvent peak was used as an internal chemical shift reference point (δC/δH 39.52/2.49). The HSQC spectra processing and data analysis were performed using the MestReNova software. The cross-peaks of the 2D HSQC NMR spectra were assigned according to prior reports.[22-23]

Thioacidolysis. Lignin monomeric composition in terms of p-hydroxyphenyl (H), guaiacyl (G), and syringyl (S) units was measured by thioacidolysis following a reported procedure[24]. The thioacidolysis reagent was freshly prepared in a 25 mL volumetric flask by adding 2.5 mL of ethanethiol, 0.7 mL of boron trifluoride diethyl etherate (BF_3 etherate), and 22.8 mL of dioxane. A 4 mL of thioacidolysis reagent was added to each of 5 mg ball milled soxhlet extracted poplar wood and lignin samples in a 5 mL high pressure vial with an aluminum crimp cap. The vial, upon purging with nitrogen and capping immediately, was hold at 100 °C for 4 h with shaking. Then the solution was quenched in an ice bath and mixed with 100 μL internal standard (tetracosane, 5 mg/mL, prepared in CH_2Cl_2). The pH of the solution was adjusted to 3-4 by adding 0.4 M $NaHCO_3$. The aqueous phase was extracted with CH_2Cl_2 for three times and the collected organic phase was dried with Na_2SO_4, and then the solvent was evaporated under reduced pressure at 40 °C. The recovered residue was dissolved in 1 mL of CH_2Cl_2. To this solution, 100 μL of BSTFA (*N,O*-Bis(trimethylsilyl)trifluoroacetamide) and 20 μL pyridine were added and the mixture was heated to 50 °C for 40 min. The silylated solution was analyzed using GC and a GC−MS following the operating conditions written below. The molecular ions and fragments of syringyl and guaiacyl units were identified based on their mass numbers following literature[24]. Quantification of lignin species was performed using the following equation:

$$W_S = (R_f \times W_{IS} \times A_S) / (A_{IS})$$

where W_S refers to the weight of the S or G unit species, W_{IS} is the mass of the Tetracosane (internal standard), A_S is the peak area of the S or G units in the chromatogram, A_{IS} is the peak area of the internal standard, and R_f = Response factor (0.53 for S, 0.47 for G)[24].

Molecular weight distribution analysis by Gel Permeation Chromatography (GPC). Generally lignin acetylation is adopted for GPC analysis due to the solubility issue but the lignin isolated from the MSH process is soluble in many organic solvents[25]. Thus lignin samples were directly dissolved in THF for GPC analysis. The lignin samples (10 mg) were dissolved in 10 mL of THF (tetrahydrofuran) and analyzed on a GPC to determine molecular weight (Mw)

distribution. The dissolved solution was filtered through syringe filters and analyzed on the Waters 2695 HPLC equipped with the RI detector (Waters model 2414). Waters Styragel HR 3 (7.8 × 300 mm × 5 μm, 500 – 30KDa) and Styragel HR 4 (7.8 × 300 mm × 5 μm, 5K– 600KDa) columns connected in series were used for the GPC separation using THF as an eluent at a rate of 0.3 mL/min. Calibration of GPC was done using polystyrene standards (WAT058931).

Lignin depolymerization. Lignin depolymerization was performed following our earlier publication.[26] Briefly, 50 mg of isolated lignin, 20 mg CoS_2 catalyst and 20 mL THF were added in a 50-mL Parr reactor with a magnetic stir bar. The reactor was equipped with a pressure gauge, a rupture disk, a pressure release valve, and an inlet. The reactor was purged three times with H_2, pressurized to 50 bar of H_2 and heated to 250 °C using a band heater at a heating rate of 10 °C min^{-1}. After 15 h of reaction time, the reactor was cooled to room temperature in an ice-bath and the gas phase was released by opening the release valve. An internal standard solution (2 mL of decane of concentration 1 mg decane/mL in heptane) was added to the reactor. The resulting mixture was filtrated through a syringe filter. The filtrate was silylated using BSFTA and pyridine under similar conditions described above and analyzed using GC and GC-MS following the operating conditions written below.

Monomer analysis by GC-MS. GC-MS analysis was performed using an Agilent 7890B series GC equipped with a HP5-MS capillary column and an Agilent 5977A series Mass Spectroscopy following our earlier publication.[24] The operating conditions for GC-MS analysis are: an injector temperature of 250 °C, an initial column temperature hold at 50 °C for 1 min followed by a ramp rate of 15 °C/min to 300 °C and hold at 300 °C for 7 min, and a detector temperature of 290 °C. Product quantification was performed on a GC (Agilent 7890B series) equipped with an HP5-column and a flame ionization detector (FID). The operating conditions for GC-FID analysis include an injector temperature 300 °C. The column temperature program was 40 °C (3 min), ramp at the rate of 30 °C/min to 100 °C, ramp at the rate of 40 °C/min to 300 °C and hold at 300 °C (5 min). The detector temperature was 300 °C. The peaks in the GC-FID chromatogram follow the patterns in the GC-MS chromatogram. Quantification was based on an internal standard (decane) and the effective carbon number (ECN) method. The monomer yield was calculated based on the area of the monomer and the area of decane in the GC chromatogram.

The calculation is as follows:

$$n_{decane} = \frac{W_{decane}}{MW_{decane}} = \frac{2\ mg}{142\ mg/mol} = 0.014\ mmol \quad (1)$$

$$n_{monomer} = \frac{A_{monomer\ in\ sample}}{A_{decane\ in\ sample}}\ X\ 0.014 mmol\ X \frac{ECN_{decane}}{ECN_{monomer}} \quad (2)$$

$$Ymonomer = \frac{n_{monomer}}{n_{monomer_{theoritical}}} X\ 100\% \quad (3)$$

Here W_{decane} (mg) is the weight of decane (internal standard) in each analyzed sample, MW_{decane} (mg mmol-1) is the molecular weight of decane (142 mg $mmol^{-1}$), n_{decane} (mmol) is the molar amount of decane in each analyzed sample, $n_{monomer}$ (mmol) is the molar amount of monomer in each analyzed sample, $A_{monomer}$ is the peak area of monomer in the GC-FID chromatogram, A_{decane} is the peak area of decane in the GC-FID chromatogram, ECN_{decane} is the effective carbon number (10) of decane, $ECN_{monomer}$ is the effective carbon number of the lignin monomer, $Y_{monomer}$ is the molar yield of monomer, W_{lignin} (mg) is the weight of the lignin, and $n_{monomer\_theoretical}$ is the theoretical lignin moles, i.e., weight (50 mg)/(220 mg/mmol)=0.227 mmol.

Acidity measurement *via* the ^{13}C-NMR probe method. ^{13}C-NMR spectra were acquired following the Fārcasiu's[27] and Rodriguez's[28] method to estimate acidity based on the change in the chemical shift of the alpha and beta carbons in mesityl oxide, a probe molecule. The spectrum was acquired on an Avance III 600 MHz NMR spectrometer (Bruker). The samples were prepared using 430 µL of the acidic solution with 20 µL of mesityl oxide (Sigma Aldrich) and 50 µL of D_2O (ACROS Organics) in NewEra quartz NMR tubes.

Thermodynamic Model (OLI Systems). pH and H^+ concentrations were calculated using the 2018 OLI software.[29] This thermodynamic model predicts the concentration and activity coefficient of species in solution by combining the standard state thermodynamic properties of the species, calculated using the Helgeson–Kirkham–Flowers (HKF), with the excess Gibbs free energy model for long, middle, and short-range interactions. The calculations were carried out using the aqueous electrolyte model of Wang et al.[29] used also in our previous work.[28]

Results and Discussion

Product Evolution in $ZnBr_2$ AMSH

First, we examined $ZnBr_2$ AMSH for the one-step depolymerization and saccharification of soxhlet extracted poplar wood at the optimal reaction conditions identified by us in LiBr AMSH.[18] All weight percent reported thereafter are based on soxhlet extracted poplar wood. Gluco-oligosaccharides form as the major product, similar to using LiBr AMSH.[18, 19] Xylo-oligosaccharides are absent in the aliquot after 30 min and the main C_5 sugar is xylose (12.5 wt%

yield; Figure 1.a and 1b), indicating that hemicellulose saccharification occurs faster than that of cellulose. The strong glycosidic interactions among glucose units make cellulose saccharification slower, affording 5.8 wt% glucose at 30 min (Figure 1.a, Table S1). The aliquot contains 43 wt% solid materials. Compositional analysis of the solid indicates 70% of the cellulose and 88% of the hemicellulose were saccharified (Table S2), i.e., the majority of saccharified cellulose is gluco-oligosaccharides. The total fraction of cellobiose (CB), cellotriose (CTr), cellotetrose (CTt), and cellopentose (CPt) is 13.5 wt%, indicating a significant amount of non HPLC-detectable gluco-oligosaccharides with a DP > 5. Further saccharification for 1 h and 3 h results in 23 and 43 wt% yield, respectively, of gluco-oligosaccharide of DP ≤ 5. The solid after 3 h reaction contains more than 99% lignin (Table S2) with traces of glucan and xylan; 87 wt% glucose and 89% xylose, based on the theoretical amount of glucan and xylan, are produced. A small fraction of levoglucosan (3 wt%) also forms. The results demonstrate that $ZnBr_2$ AMSH is as efficient as LiBr AMSH[13] in producing high yield of soluble sugars in one step without pretreatment and has the potential to make upstream sugar production less costly.

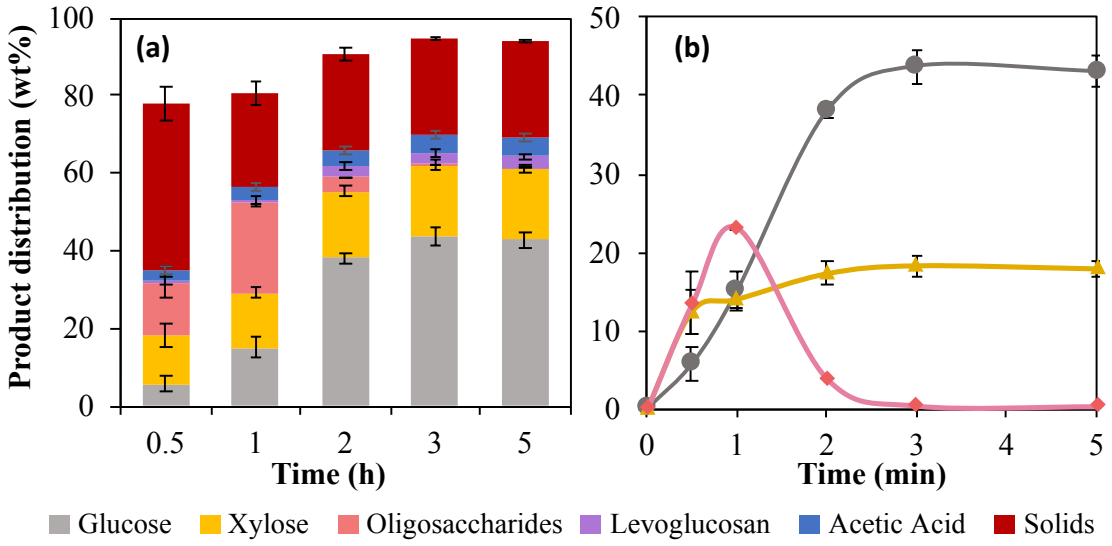

Figure 1. Soluble and solid products in one-step soxhlet extracted poplar wood depolymerization and saccharification in $ZnBr_2$ AMSH. (a) Yields of all products, based on soxhlet extracted poplar wood dry weight, as a function of reaction time (Table S1 tabulates yields of glucose and xylose on the basis of theoretical glucan and xylene in poplar wood). HMF≤0.3%, furfural≤1%, and acid soluble lignin≤0.8% are not shown. (b) Time profiles for glucose, xylose and gluco-oligosaccharides. Reaction conditions: 3.45 wt% soxhlet extracted poplar wood, 73 wt% $ZnBr_2$, water/salt molar ratio 4, 2.25 mL 0.05 M H_2SO_4, 85 °C.

Product Evolution in $ZnBr_2$ MSH

Next, we studied one-step soxhlet extracted poplar wood depolymerization and saccharification in $ZnBr_2$ MSH (without H_2SO_4 acid). At comparable conditions, the $ZnBr_2$ MSH medium achieves 70 wt% glucose and 89 wt% xylose yields in 3 h based on the theoretical amounts (35 wt% glucose and 15 wt% xylose on soxhlet extracted poplar wood basis), as shown in Figure 2a. The solid consists mainly of lignin, indicating complete depolymerization of soxhlet extracted poplar wood and the remaining cellulose and hemicellulose components of soxhlet extracted poplar wood were present as soluble sugars (monomeric and oligomeric) in the MSH phase. All products are the same in MSH as in AMSH except for a lower yield of glucose (grey bar) and a higher yield to oligomers. This discovery is significant as a non-acidified media could (1) minimize lignin re-condensation, (2) give cost-savings, and (3) eliminate complex separations of acid from the hydrolysate.

Figure 2 b and c compare the glucose and xylose yields vs. time in $ZnBr_2$ MSH and AMSH media. An initial induction period of 1 h occurs in the $ZnBr_2$ MSH. After this induction period, the reaction accelerates and follows the time profile of the $ZnBr_2$ AMSH system. The long-time yields are comparable in both media. Previous studies in acidified salt solutions have shown that it often takes time for the pH to equilibrate.[30] To assess whether pH equilibration is responsible for the induction period, the $ZnBr_2$ MSH solution was preheated at reaction temperature for 1 h before adding soxhlet extracted poplar wood (Figure S1). A similar induction period is seen. Given this finding, the induction period in glucose, but not in xylose, suggests that it is caused by the longer time to exfoliate and dissolve the crystalline cellulose polymer compared to the amorphous hemicellulose and points to an important role of H_2SO_4 in the AMSH.

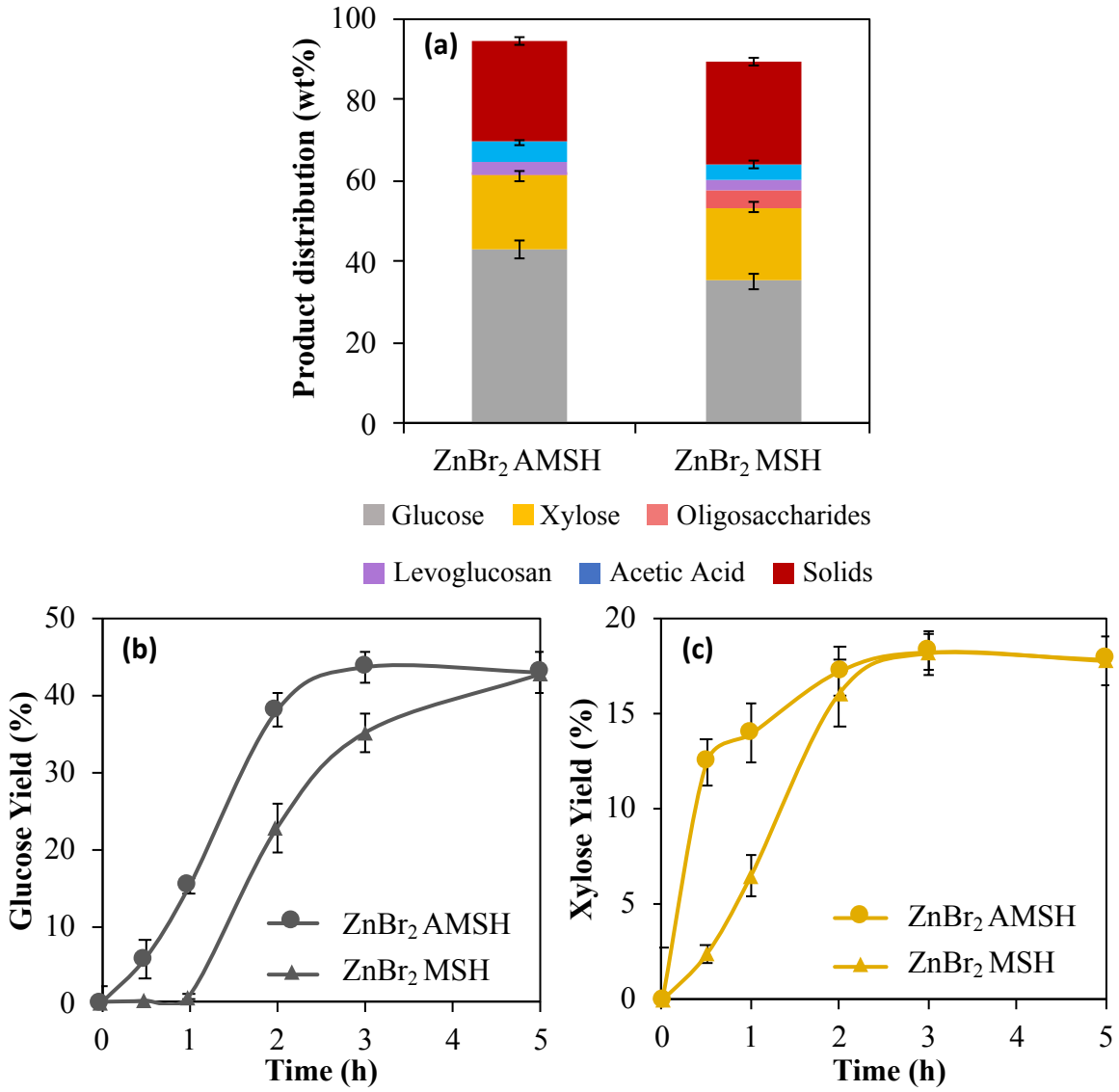

Figure 2. (a) Soluble and solid products in one-step depolymerization and saccharification of soxhlet extracted poplar wood in $ZnBr_2$ MSH and $ZnBr_2$ AMSH media at 3 h. HMF≤0.3%, furfural≤1%, and acid soluble lignin≤0.8% are not shown. (b) Glucose and (c) xylose yields in one-step depolymerization and saccharification of SEPW in $ZnBr_2$ MSH and $ZnBr_2$ AMSH media. Reaction conditions: 3.45 wt% soxhlet extracted poplar wood, water to $ZnBr_2$ molar ratio 4 and 85 °C. Yields are on dry weight of SEPW.

On the Origin of Acidity of $ZnBr_2$ AMSH and $ZnBr_2$ MSH

In previous work,[14] we showed that the Hammett effective acidity and the electrode potential method have drawbacks in quantifying the acidity of the LiBr AMSH medium due to the non-ideality of concentrated high ionic strength solutions. We demonstrated that C^{13} NMR

spectroscopy is effective for comparing the acidity of various solutions. Furthermore, thermodynamic calculations (OLI systems) rationalized that the super acidity of LiBr AMSH[28] stems from complete de-protonation of the sulfuric acid (increasing the H^+ concentration), complexation between the acid ions and the Li^+ ions that drive dissociation of LiBr, and an increase in the H^+ activity due to non-ideal behavior of the media.[28] The anions of the salt enhance the acidity by deshielding the hydronium cations that tend to leave water.[31-33] The model was able to rationalize results for various inorganic acids and metal salts and demonstrated that a small concentration of H_2SO_4 is essential to create a super acidic media. Observed differences among salts and acids arrive mainly from differences in acidity (pH).

To understand the difference in reactivity between the $ZnBr_2$ AMSH and $ZnBr_2$ MSH systems, we calculated the pH of both solutions vs. $ZnBr_2$ concentration and compare it also to that of LiBr. We start with comparing the two $ZnBr_2$ solutions. Although both solutions are highly acidic (Figure 3a), the AMSH solution has a lower pH, which explains the faster rate of

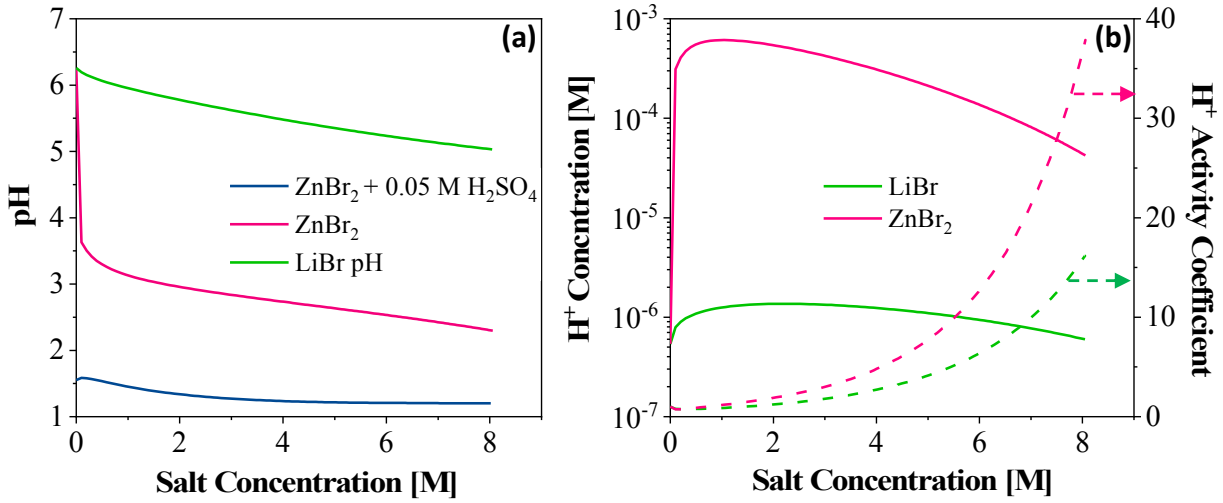

Figure 3. (a) Effect of $ZnBr_2$ concentration on the pH of solutions ($ZnBr_2$ MSH and $ZnBr_2$ AMSH) calculated using OLI at 85 °C. (b) Activity coefficient for LiBr and $ZnBr_2$ salts in dashed lines (right axis) and proton concentration in solid lines (left axis) calculated using the OLI model at 85 °C. $ZnBr_2$ MSH corresponds to 76 wt% equivalent to 8 M $ZnBr_2$. LiBr MSH occurs at 58 wt% equivalent to 11.2 M.

saccharification with the addition of a small amount of acid.

To understand the effect of temperature on acidity, we calculated the pH as a function of temperature (Figure S2). Figure S2 shows that with increasing temperature (from 25 °C to 100

°C), the pH of the $ZnBr_2$ MSH solution decreases while the pH of the $ZnBr_2$ AMSH increases. This suggests that MSH becomes more effective at higher reaction temperatures. Finally, we compared the protonating ability of the two media at room temperature using NMR. We correlate the change in the chemical shift of the beta carbon of the protonated mesityl oxide in the acidified solutions with respect to the non-protonated mesityl oxide in deuterated chloroform to the acidity of the solution. Figure S3a-c show that the $ZnBr_2$ MSH and $ZnBr_2$ AMSH at room temperature have comparable protonating power. Furthermore, the protonating ability of these systems is comparable to that of a solution of 8 M LiBr in 0.05 M H_2SO_4 (LiBr AMSH) (Figure S3d). Of course, these comparisons are made at room temperature, and thus, are a rough indicator of acidity, given that the pH changes with temperature (Figure S2), but they, in general, support experimentally the fact that $ZnBr_2$ is an effective media.

Unlike previous reports that found the best performing MSH to require an inorganic acid,[15, 30] we have shown that $ZnBr_2$ MSH is capable of one-step depolymerization and saccharification of soxhlet extracted poplar wood. It is worth mentioning that the acidity of the solution may be affected by the basic metals present in some biomasses with high ash content, such as corn stover and switch grass. The proposed literature mechanism[34] shows that the Lewis acidic nature of zinc helps the breakdown of the glycosidic linkage in cellulose. To understand why $ZnBr_2$ MSH does not require an acid, we compared the pH as a function of salt concentration of the LiBr and $ZnBr_2$ MSH. Figure 3a shows that $ZnBr_2$ MSH is significantly more acidic than LiBr MSH. Figure 3b shows that addition of $ZnBr_2$ in water results in hydronium cations (H^+) while LiBr does not affect the H^+ concentration. Furthermore, although both salts increase the H^+ activity coefficient, $ZnBr_2$ increases it more at lower pH (higher salt concentration). Although the H^+ concentration decreases at higher salt concentration, the activity coefficient of the hydronium cations increases monotonically explaining the overall decrease in pH. For the LiBr, although the H^+ concentration does not change significantly with salt concentration, the increase in the activity coefficient results in an overall decrease in the pH but to a less extent than the $ZnBr_2$ system.

The sharp increase in proton concentration and decrease in pH at low concentrations of $ZnBr_2$ can be attributed to the inherent Brønsted acidic nature of the formed metal aqua species in solution (Eq. 4)[35]

$$M(H_2O)_n^{x+} + y\ H_2O \leftrightarrow M(H_2O)_{n-y}(OH)_y^{(x-y)+} + y\ H_3O^+ \qquad (4)$$

The strong interaction between the Lewis acidic zinc cation (Zn^{2+}) and the oxygen atom in the coordinated water molecules results in the hydrolysis of the metal aquo complex, through weakening of the O-H bond, deprotonating the coordinated water (Eq. 4).[36] In contrast, the poor Lewis acidity of the lithium cation results in low concentration of Brønsted acid species from the coordinated water molecules, explaining the negligible effect of LiBr on the proton concentration and therefore the higher pH.

Structure of isolated lignin

The structure of isolated lignin depends largely on the depolymerization conditions of biomass,[9, 37-38] due to the varying degree of re-condensation of soluble lignin species during depolymerization. Prior reports by us[26, 39] and others suggest that the native lignin in biomass contains ~55-60% of C−O inter-unit linkages including β-O-4 bonds. In contrast, the technical lignin (isolated lignin from cellulosic biorefineries or paper pulping processes) has a high degree of C−C linkages, owing to re-condensation.[26, 39-42] High bond dissociation energies (BDEs) of C−C linkages, in comparison to C−O linkages, has been hypothesized to make depolymerization of the technical lignin ineffective at conditions at which the C−O bonds are selectively cleaved.[41-44] However, the BDE concepts is limited as it does not include information on the conformation of adsorbed species and new pathways introduced by the catalyst.

We used 2D $^{13}C–^{1}H$ HSQC NMR to analyze linkages[22] in lignin isolated from one-step soxhlet extracted poplar wood depolymerization and saccharification in $ZnBr_2$ MSH and $ZnBr_2$ AMSH media. Figure 4 shows no signals in the polysaccharide anomeric region (δC/δH 90–105/3.9–5.4) indicating absence of sugar-lignin linkages. In the sidechain region, the AMSH lignin shows signals characteristic of aromatic methoxy (Ar-OMe) and of β–β linkages but not of β-O-4 linkages (Figure 4a). In contrast, the MSH lignin has β-O-4, aromatic methoxy (Ar-OMe), and β–β linkages (Figure 4b). This finding is significant for a number of reasons: (1) β-O-4 linkages, containing S and G lignin subunits (Table 1) of lower BDEs than those of C−C linkages, can be cleaved selectively and effectively to functional phenols at mild conditions, and (2) $ZnBr_2$ alters less the structure of the native lignin of biomass by retaining some of the β-O-4 linkages.

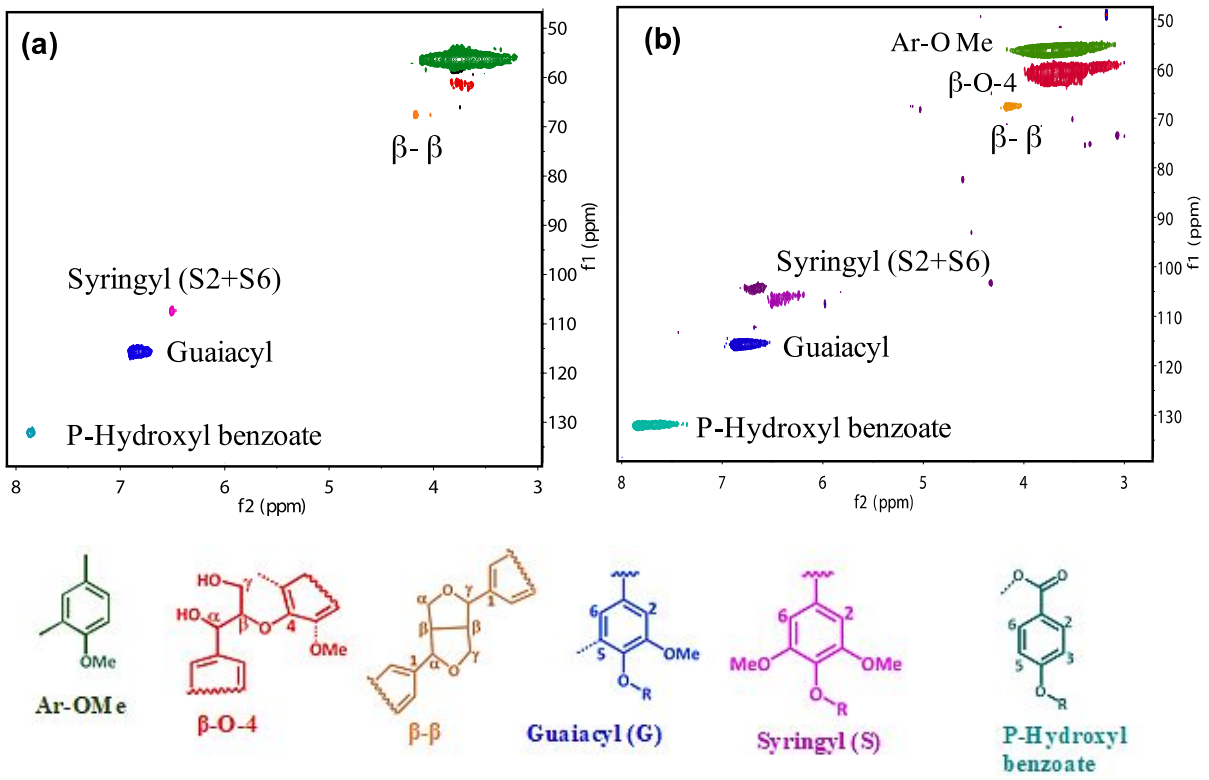

Figure 4. 2D HSQC NMR of isolated lignins from one-step SEPW depolymerization and saccharification in (a) $ZnBr_2$ AMSH and (b) $ZnBr_2$ MSH media. The NMR signals in red color show the presence of β-O-4 linkages in $ZnBr_2$ MSH lignin.

The signal strength for the Cα-Hα cross peak and the Cβ-Hβ cross peak used for the semi-quantitative analysis of the β-O-4 linkage and the beta-beta linkage is low for the lignin samples making semi-quantitative analysis challenging. The thioacidolysis method was followed[24] to quantify the β-O-4 linkages (Table 1). First, S and G lignin subunits of raw poplar wood (PW) were determined; the relative distributions of S and G units obtained are in close agreement with those of the literature values of 63 S units and 37 G units.[45] We find 8.4% β-O-4 linkages in MSH and a few β-O-4 bonds in AMSH lignin. Comparison of the β-O-4 linkages in native lignin and MSH lignin shows that only 17.4% of the native β-O-4 linkages are retained in MSH lignin and the remaining 82.6% β-O-4 linkages are condensed. These results indicate that the MSH lignin is still more condensed compared to native lignin but it is less condensed compared to acidified lignin. The difference from the 2D NMR data may arise from experimental uncertainly of either the NMR method or the thioacidolysis.

Table 1. Yields (in μmol g-1 lignin) of monomeric guaiacyl (G) and syringyl (S) products from thioacidolysis of PW lignin and isolated lignin samples.

Lignin sample	Yield (μmole/g lignin)			S/G	β-O-4 (wt%)
	S	G	S+G		
Poplar wood	1121.6 ± 84.4	771.9 ± 97.5	1893.5 ± 13.0	1.5 ± 0.3	48.4 ± 0.1
MSH-based	193.7	136.1	329.8	1.4	8.4
AMSH-based	38.1	37.8 ~~9~~	75.9	1.0	1.9

GPC analysis (Figure S4) shows that both lignins have similar Mw distribution profiles with the AMSH sample having a slightly lower average Mw (2150 Da) compared to MSH one (2590 Da).

Catalytic depolymerization of lignins

Catalytic depolymerization of lignin was performed using a commercial CoS_2 catalyst following our recent work.[26] The reason behind choosing CoS_2 over Ru/C for the lignin depolymerization is the efficiency of the former towards C-C cleavage[26]. Wei et al.[46] investigated the C-C cleavage mechanism over metal sulfides focusing on FeS_2 for diphenylmethane cracking and reported that FeS_2 plays an important role in the formation of H atoms under H_2 pressure and the addition of these H atoms to the ipso position of diphenylmethane leads to the cleavage of the $C_{aromatic}$-C_{alkyl} bond. The AMSH lignin sample, containing minimal β-O-4 linkages, yields only 1.3% aromatic monomers, namely 0.5% of phenol (compound A in Figure 5) and 0.8% catechol (compound B in Figure 5), likely via C−C cleavage. In contrast, the MSH lignin, containing a higher fraction of β-O-4 linkages, results in

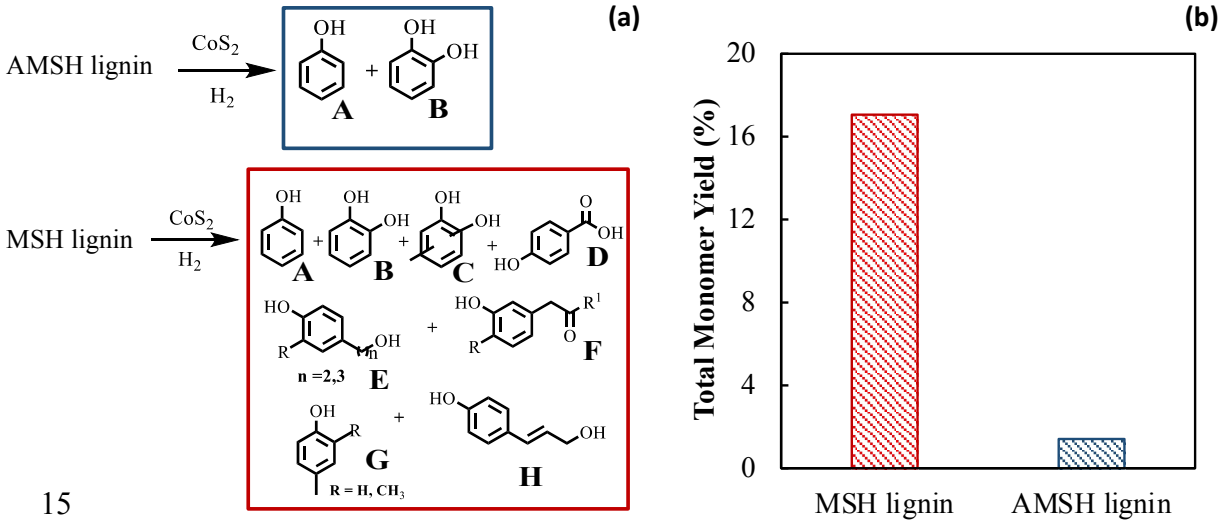

Figure 5. (a) Structures of aromatic monomers from lignin. (b) Total monomer yields from catalytic depolymerization over CoS_2. Reaction conditions: 50 mg lignin, 50 mg CoS_2, 20 mL THF (solvent), 50 bar H_2, 250 °C, 15 h. The optimal reaction conditions in our prior work[24] were used here.

17% total monomers (A= 0.8%, B= 1.2%, C= 3.9%, D= 1.8%, E= 1.1%, F = 6.7%, G= 1.2%, H= 0.4%) (Figure 5). The yield of each monomer is given in Table S3 and Figure S5. The monomer yields achieved from the MSH lignin are higher than those from the kraft lignin (12.6%) depolymerization under the same conditions over CoS_2 in our previous work. These monomer yields corroborate with the higher percentage β-O-4 content in the MSH lignin (Table 1) and are consistent with prior reports by us and others.[47]

Figure 6a and 6b show the Mw distribution of the solutions obtained by GPC. The distribution for the MSH lignin is narrower (Figure 6b), indicating a higher degree of depolymerization, consistent with the higher amounts of total monomer yield.

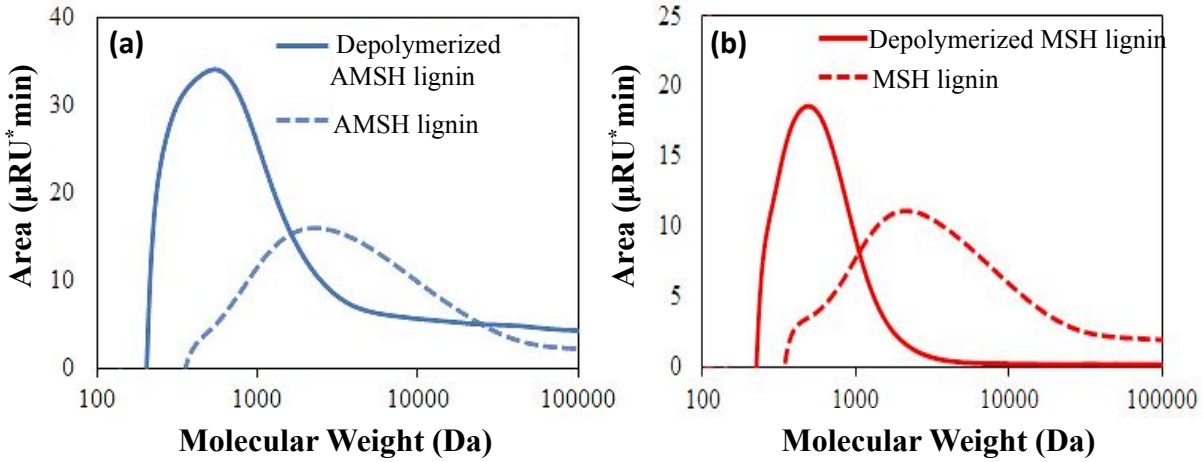

Figure 6. GPC molecular weight distribution of depolymerized lignin species for (a) AMSH and (b) MSH. Dashed lines correspond to unpolymerized lignin. Reaction conditions of 50 mg lignin, 50 mg CoS_2, 20 mL THF (solvent), 50 bar H_2, 250 °C, 15 h.

To further assess the quality of the MSH lignin, a typical reductive catalytic fraction (RCF) of AMSH lignin and MSH lignin was performed over Ru/C and compared with the RCF of the whole poplar wood. The RCF conditions were selected from a recent report by our group. Each monomer yield and the total monomer yield from the whole poplar wood, the acidified MSH lignin and the no acid MSH lignin are given in Table S4. The GC chromatogram for the whole poplar wood after RCF and the chemical structure of the monomers is shown in Figure S6. RCF results indicate that the total monomer yield for the MSH treated lignin (20.6% for MSH lignin and 9.7% for AMSH lignin) were lower than that of whole poplar wood (49.4%) based on the lignin weight. The MSH lignin resulted in two times higher total monomer yield compared to the

AMSH lignin indicating the improved quality of lignin in the absence of acid using the MSH process.

Techno-economic analysis (TEA)

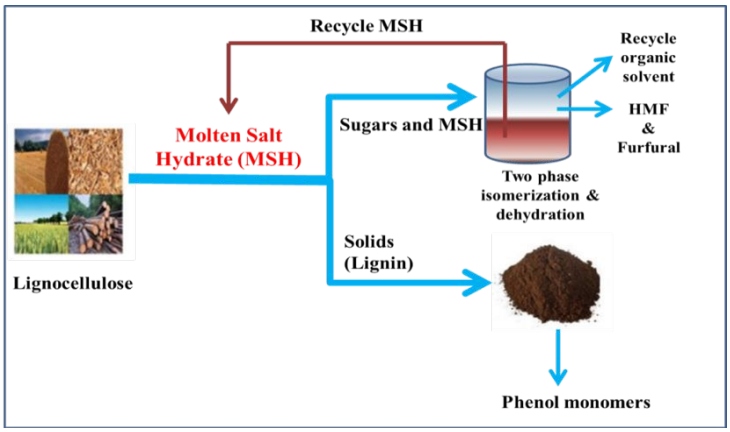

Figure 7. Illustration of integrated biomass saccharification and dehydration of sugars in biomass hydrolyzate considered for techno economic analysis.

In our recent work[13] with LiBr molten salt hydrate (MSH), we demonstrated an integrated approach for the separation of sugars in the form of furfurals (HMF and furfural) in a biphasic system. This approach enabled concurrent reactive extraction of furfurals into an extraction solvent and recycling of the reactive MSH phase. This process intensification approach addressed both sugar separation as well as furfural production in an integrated manner. This approach can be applied to the current $ZnBr_2$ MSH process to separate and recycle $ZnBr_2$ MSH phase. The concentration of zinc salt in the end product HMF is expected to be within the safety limitations (Sigma Aldrich ZnBr2 SDS data -Acute toxicity, LD50 Oral - Rat - 1,447 mg/kg (0.1447%) as per our learning from LiBr MSH process. Figure 7 illustrates the integrated biomass saccharification and dehydration of sugars in biomass hydrolyzate considered for techno-economic analysis.

Using our experimental glucose yield from the $ZnBr_2$ AMSH and MSH and the HMF recovery results from glucose dehydration following our prior work as mentioned above,[18] we performed TEA for HMF production using the Aspen Economic analyzer V8.8. The NRTL thermodynamic package was utilized to predict the liquid−liquid and liquid−vapor behavior.[48] Process flowsheets for our MSH processes and other literature hydrolysis processes (*e.g.*, dilute acid and concentrated acid processes) and HMF production from hydrolyzed glucose are shown in Figures S7 and S8. The process description is in the supporting information. Components are

directly selected from the Aspen database[49-50] and when missing (e.g., lignin, hemi-cellulose, etc.), they were defined using structures and properties of NREL.[51] The production cost of HMF was used to determine the minimum cost, which is defined as the selling price of the product when the net present value (NPV) is zero.[52] All the equipment and operating costs are based on prices of the first quarter in 2014. The composition of biomass was taken from the experimental data and biomass processing capacity of the biorefinery was assumed as 50 metric tons per hour. The biomass loading is assumed as 10 wt%. The current experimental studies are limited to 3.45% biomass loading due to stirring limitations[13] of such a highly viscosity of molten salt hydrate system that lowers glucose yields. However, higher biomass loadings (≥ 15%) are feasible as evidenced in the literature[53].The average cost of biomass is assumed as $60 per ton.[54]

Table 2. Total amount of products produced in AMSH and MSH process.

Process	AMSH	MSH
HMF Produced (ton/yr)	103,478	95,038
Furfural Produced (ton/yr)	67,803	64,038
Purity of furans	99%	99%
Lignin Produced (ton/yr)	134,074	152,671
Purity of lignin	85%	77%

Products from both processes are listed in Table 2. For the base case scenario, we assumed electricity production from both processes by burning lignin. The capital and operating costs of the AMSH process are estimated at $176 million and $51.6 million, respectively vs. $182 million and $53 million of the MSH process, respectively (Figure 8). The longer reaction time of the MSH process contributes to a slightly higher capital cost compared with the AMSH process. The operating cost of both processes is similar. This finding points to the sensitivity of the cost on processing time and the need to find ways to intensify the process and reduce processing time.

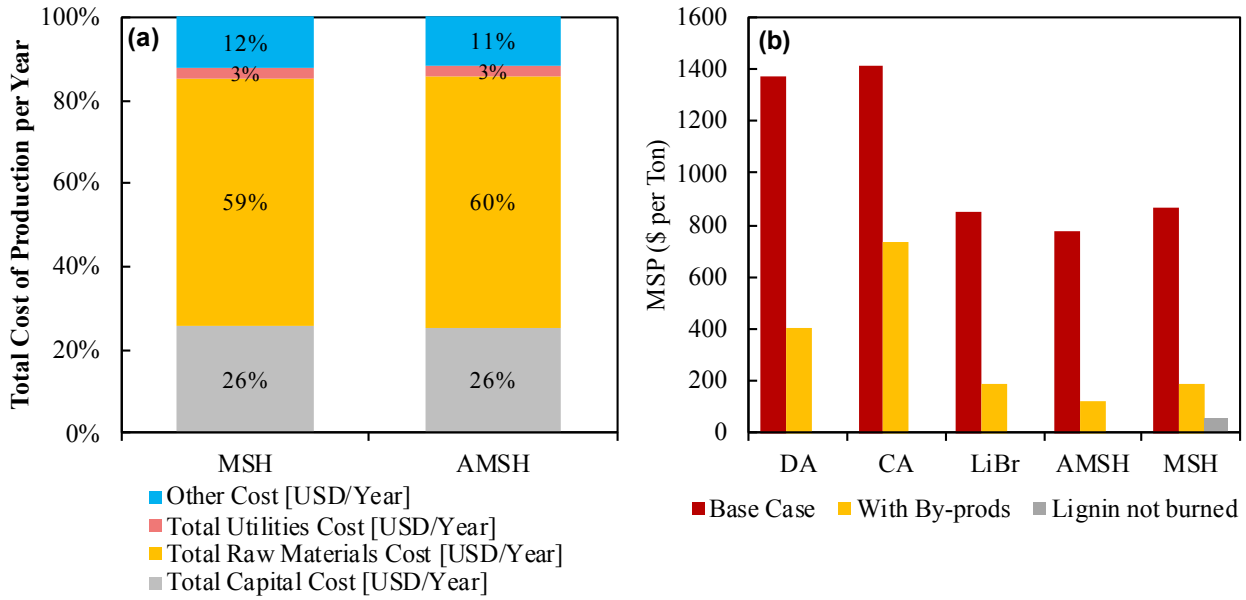

Figure 8. Comparison of a) capex and variable costs for HMF production from biomass from dilute acid (DA) hydrolysis, concentrated acid (CA) hydrolysis, $ZnBr_2$ AMSH and $ZnBr_2$ MSH and b) corresponding minimum sales price (MSP) of HMF/metric ton. DA=dilute acid hydrolysis; CA=concentrated acid hydrolysis; LiBr corresponds to AMSH media; AMSH and MSH correspond to $ZnBr_2$.

The minimum selling prices of HMF from $ZnBr_2$ AMSH and $ZnBr_2$ MSH were compared to conventional hydrolysis processes (Figure 8b). When furfural is considered and lignin is used to generate electricity, the minimum price of HMF is \$776 per metric ton for the $ZnBr_2$ AMSH process and \$865 per metric ton for the $ZnBr_2$ MSH process. When a price of furfural of \$1,000 per metric ton is considered, the minimum price of HMF decreases to \$120 and \$191 per metric ton for the $ZnBr_2$ AMSH and MSH process, respectively. Clearly, co-production and use of furfural has a huge impact on economics. The market price of lignin is estimated to range between \$100 per metric ton to \$250 per metric ton based on purity.[55] For a lignin price of \$100 per metric ton, the minimum price of HMF produced using the $ZnBr_2$ MSH process further decreases to \$60 per metric ton. The breakdown costs are given in Table S5, S6 and Figure S9. The mass balance for the hydrolysis and dehydration steps of the MSH process are given in Table S7. We believe that the value of the specific monomers made from lignin can even be higher. However, suitable separation and conversion technologies need to be developed and the TEA be revisited.

Conclusions

We reported an effective strategy for one-step depolymerization and saccharification of raw Soxhlet Extracted Poplar Wood to obtain high sugar yield and isolated lignin that exhibits significantly less C-C condensation. $ZnBr_2$, at molten salt hydrate (MSH) conditions acidified with a small amount of H_2SO_4 ($ZnBr_2$ AMSH), enables the direct conversion of soxhlet extracted poplar wood to 88% glucose and 89% xylose based on theoretical amounts of glucan and xylan, with lignin being the only solid product. Similar sugar yields are achieved in $ZnBr_2$ MSH (without added acid) but at longer times. Thermodynamic modeling and ^{13}C NMR spectroscopy support a picture where the stronger Lewis acid character of the Zn^{2+} cation enables the deprotonation of the coordinated water molecules, resulting in a higher acidity compared to LiBr MSH. The increased acidity stems mainly from the increase in the activity coefficient of the hydronium ions promoted by the high ionic strength at high salt concentrations.

The isolated MSH lignin contains 8.4% C−O linkages compared to the AMSH lignin that contains 1.8% C-O linkages, as evidenced by 2D HSQC NMR. The catalytic depolymerization of isolated MSH lignin over CoS_2 catalyst achieves 17% yield to phenol monomers compared to only 1% from the AMSH lignin. Techno-economic analysis exposes favorable economics of the $ZnBr_2$ process compared to traditional hydrolysis biomass saccharification processes, with the MSH process being very appealing due to the potential of utilizing the lignin. This can enable cellulosic sugar production economically viable, which is the key step to make downstream bioproducts cost-competitive

Conflicts of Interest

There are no conflicts of interest to declare.

Acknowledgements

This work was supported as part of the Catalysis Center for Energy Innovation, an Energy Frontier Research Center funded by the U.S. Department of Energy, Office of Science, Office of Basic Energy Sciences under Award Number DE-SC0001004. The authors thank James Sheehan, postdoctoral researcher at the Catalysis Center for Energy Innovation for further evaluating and providing helpful insights into the 2D HSQC NMR characterizations of the lignin samples.

References

1. Hess, J. R.; Foust, T. D.; Hoskinson, R.; Thompson, D. *Roadmap for agriculture biomass feedstock supply in the United States*; Department of Energy (DOE): 2003.
2. Huber, G. W.; Iborra, S.; Corma, A., Synthesis of transportation fuels from biomass: chemistry, catalysts, and engineering. *Chemical reviews* **2006,** *106* (9), 4044-4098.
3. Luque, R.; Herrero-Davila, L.; Campelo, J. M.; Clark, J. H.; Hidalgo, J. M.; Luna, D.; Marinas, J. M.; Romero, A. A., Biofuels: a technological perspective. *Energy & Environmental Science* **2008,** *1* (5), 542-564.
4. Dapsens, P. Y.; Mondelli, C.; Pérez-Ramírez, J., Biobased chemicals from conception toward industrial reality: lessons learned and to be learned. *Acs Catalysis* **2012,** *2* (7), 1487-1499.
5. Tuck, C. O.; Pérez, E.; Horváth, I. T.; Sheldon, R. A.; Poliakoff, M., Valorization of biomass: deriving more value from waste. *Science* **2012,** *337* (6095), 695-699.
6. Sanford, K.; Chotani, G.; Danielson, N.; Zahn, J. A., Scaling up of renewable chemicals. *Current opinion in biotechnology* **2016,** *38*, 112-122.
7. Alvira, P.; Tomás-Pejó, E.; Ballesteros, M.; Negro, M., Pretreatment technologies for an efficient bioethanol production process based on enzymatic hydrolysis: a review. *Bioresource technology* **2010,** *101* (13), 4851-4861.
8. Singh, S.; Cheng, G.; Sathitsuksanoh, N.; Wu, D.; Varanasi, P.; George, A.; Balan, V.; Gao, X.; Kumar, R.; Dale, B. E., Comparison of different biomass pretreatment techniques and their impact on chemistry and structure. *Frontiers in Energy Research* **2015,** *2*, 62.
9. Sturgeon, M. R.; Kim, S.; Lawrence, K.; Paton, R. S.; Chmely, S. C.; Nimlos, M.; Foust, T. D.; Beckham, G. T., A mechanistic investigation of acid-catalyzed cleavage of aryl-ether linkages: implications for lignin depolymerization in acidic environments. *ACS Sustainable Chemistry & Engineering* **2014,** *2* (3), 472-485.
10. Sannigrahi, P.; Ragauskas, A. J., Characterization of fermentation residues from the production of bio-ethanol from lignocellulosic feedstocks. *Journal of Biobased Materials and Bioenergy* **2011,** *5* (4), 514-519.
11. Shimada, K.; Hosoya, S.; Ikeda, T., Condensation reactions of softwood and hardwood lignin model compounds under organic acid cooking conditions. *Journal of wood chemistry and technology* **1997,** *17* (1-2), 57-72.
12. Liao, Y.; Koelewijn, S.-F.; Van den Bossche, G.; Van Aelst, J.; Van den Bosch, S.; Renders, T.; Navare, K.; Nicolaï, T.; Van Aelst, K.; Maesen, M., A sustainable wood biorefinery for low–carbon footprint chemicals production. *Science* **2020,** *367* (6484), 1385-1390.
13. Sadula, S.; Athaley, A.; Zheng, W.; Ierapetritou, M.; Saha, B., Process intensification for cellulosic biorefineries. *ChemSusChem* **2017,** *10* (12), 2566-2572.
14. Sadula, S.; Oesterling, O.; Nardone, A.; Dinkelacker, B.; Saha, B., One-pot integrated processing of biopolymers to furfurals in molten salt hydrate: understanding synergy in acidity. *Green Chemistry* **2017,** *19* (16), 3888-3898.
15. Deng, W.; Kennedy, J. R.; Tsilomelekis, G.; Zheng, W.; Nikolakis, V., Cellulose hydrolysis in acidified libr molten salt hydrate media. *Industrial & Engineering Chemistry Research* **2015,** *54* (19), 5226-5236.
16. Chen, L. F.; Yang, C.-M., Quantitative hydrolysis of cellulose to glucose using zinc chloride. Google Patents: 1984.
17. de Almeida, R. M.; Li, J.; Nederlof, C.; O'Connor, P.; Makkee, M.; Moulijn, J. A., Cellulose conversion to isosorbide in molten salt hydrate media. *ChemSusChem: Chemistry & Sustainability Energy & Materials* **2010,** *3* (3), 325-328.

18. Sen, S.; Martin, J. D.; Argyropoulos, D. S., Review of cellulose non-derivatizing solvent interactions with emphasis on activity in inorganic molten salt hydrates. *ACS Sustainable Chemistry & Engineering* **2013,** *1* (8), 858-870.
19. Cao, N.; Xu, Q.; Chen, L., Acid hydrolysis of cellulose in zinc chloride solution. *Applied Biochemistry and Biotechnology* **1995,** *51* (1), 21.
20. Penque, R. A., Method of hydrolyzing cellulose to monosaccharides. Google Patents: 1977.
21. Sluiter, A.; Hames, B.; Ruiz, R.; Scarlata, C.; Sluiter, J.; Templeton, D.; Crocker, D., Determination of structural carbohydrates and lignin in biomass. *Laboratory analytical procedure* **2008,** *1617* (1), 1-16.
22. Zhang, L.; Yan, L.; Wang, Z.; Laskar, D. D.; Swita, M. S.; Cort, J. R.; Yang, B., Characterization of lignin derived from water-only and dilute acid flowthrough pretreatment of poplar wood at elevated temperatures. *Biotechnology for biofuels* **2015,** *8* (1), 203.
23. Wen, J.-L.; Sun, S.-L.; Xue, B.-L.; Sun, R.-C., Recent advances in characterization of lignin polymer by solution-state nuclear magnetic resonance (NMR) methodology. *Materials* **2013,** *6* (1), 359-391.
24. Dence, C. W., The determination of lignin. In *Methods in lignin chemistry*, Springer: 1992; pp 33-61.
25. Li, N.; Pan, X.; Alexander, J., A facile and fast method for quantitating lignin in lignocellulosic biomass using acidic lithium bromide trihydrate (ALBTH). *Green Chemistry* **2016,** *18* (19), 5367-5376.
26. Shuai, L.; Sitison, J.; Sadula, S.; Ding, J.; Thies, M. C.; Saha, B., Selective C–C bond cleavage of methylene-linked lignin models and kraft lignin. *Acs Catalysis* **2018,** *8* (7), 6507-6512.
27. Fărcaşiu, D.; Ghenciu, A., Determination of acidity functions and acid strengths by 13C NMR. *Progress in Nuclear Magnetic Resonance Spectroscopy* **1996,** *29* (3-4), 129-168.
28. Rodriguez Quiroz, N.; Padmanathan, A. M.; Mushrif, S. H.; Vlachos, D. G., Understanding Acidity of Molten Salt Hydrate Media for Cellulose Hydrolysis by Combining Kinetic Studies, Electrolyte Solution Modeling, Molecular Dynamics Simulations, and 13C NMR Experiments. *ACS Catalysis* **2019,** *9* (11), 10551-10561.
29. Wang, P.; Anderko, A.; Young, R. D., A speciation-based model for mixed-solvent electrolyte systems. *Fluid Phase Equilibria* **2002,** *203* (1-2), 141-176.
30. Rodriguez Quiroz, N.; Norton, A. M.; Nguyen, H.; Vasileiadou, E.; Vlachos, D. G., Homogeneous Metal Salt Solutions for Biomass Upgrading and Other Select Organic Reactions. *ACS Catalysis* **2019,** *9* (11), 9923-9952.
31. Emons, H.-H., Structure and properties of molten salt hydrates. *Electrochimica acta* **1988,** *33* (9), 1243-1250.
32. Sare, E.; Moynihan, C.; Angell, C., Proton magnetic resonance chemical shifts and the hydrogen bond in concentrated aqueous electrolyte solutions. *The Journal of Physical Chemistry* **1973,** *77* (15), 1869-1876.
33. Duffy, J.; Ingram, M., Acidic nature of metal aquo complexes: Proton-transfer equilibriums in concentrated aqueous media. *Inorganic Chemistry* **1978,** *17* (10), 2798-2802.
34. Amarasekara, A. S.; Ebede, C. C., Zinc chloride mediated degradation of cellulose at 200 C and identification of the products. *Bioresource technology* **2009,** *100* (21), 5301-5304.
35. Mesmer, R.; Baes, C., Review of Hydrolysis Behavior of Ions in Aqueous Solutions. *MRS Online Proceedings Library Archive* **1990,** *180*.

36. Baes, C.; Mesmer, R., The Hydrolysis of Cations. John Wiley & Sons, New York, London, Sydney, Toronto 1976. 489 Seiten, Preis:£ 18.60. *Berichte Bunsenges Für Phys Chem* **1977,** *81*, 245-246.
37. Trajano, H. L.; Engle, N. L.; Foston, M.; Ragauskas, A. J.; Tschaplinski, T. J.; Wyman, C. E., The fate of lignin during hydrothermal pretreatment. *Biotechnology for biofuels* **2013,** *6* (1), 110.
38. Shuai, L.; Yang, Q.; Zhu, J.; Lu, F.; Weimer, P.; Ralph, J.; Pan, X., Comparative study of SPORL and dilute-acid pretreatments of spruce for cellulosic ethanol production. *Bioresource Technology* **2010,** *101* (9), 3106-3114.
39. Shuai, L.; Amiri, M. T.; Luterbacher, J. S., The influence of interunit carbon–carbon linkages during lignin upgrading. *Current Opinion in Green and Sustainable Chemistry* **2016,** *2*, 59-63.
40. Bouxin, F. P.; McVeigh, A.; Tran, F.; Westwood, N. J.; Jarvis, M. C.; Jackson, S. D., Catalytic depolymerisation of isolated lignins to fine chemicals using a Pt/alumina catalyst: part 1—impact of the lignin structure. *Green Chemistry* **2015,** *17* (2), 1235-1242.
41. Wang, X.; Rinaldi, R., Solvent effects on the hydrogenolysis of diphenyl ether with Raney nickel and their implications for the conversion of lignin. *ChemSusChem* **2012,** *5* (8), 1455-1466.
42. Rinaldi, R.; Palkovits, R.; Schüth, F., Depolymerization of cellulose using solid catalysts in ionic liquids. *Angewandte Chemie International Edition* **2008,** *47* (42), 8047-8050.
43. Younker, J. M.; Beste, A.; Buchanan Iii, A., Computational Study of Bond Dissociation Enthalpies for Substituted β-O-4 Lignin Model Compounds. *ChemPhysChem* **2011,** *12* (18), 3556-3565.
44. Parthasarathi, R.; Romero, R. A.; Redondo, A.; Gnanakaran, S., Theoretical study of the remarkably diverse linkages in lignin. *The Journal of Physical Chemistry Letters* **2011,** *2* (20), 2660-2666.
45. Tolbert, A.; Akinosho, H.; Khunsupat, R.; Naskar, A. K.; Ragauskas, A. J., Characterization and analysis of the molecular weight of lignin for biorefining studies. *Biofuels, Bioproducts and Biorefining* **2014,** *8* (6), 836-856.
46. Wei, X. Y.; Ogata, E.; Zong, Z. M.; Niki, E., Effects of hydrogen pressure, sulfur, and iron sulfide (FeS2) on diphenylmethane hydrocracking. *Energy & Fuels* **1992,** *6* (6), 868-869.
47. Si, X.; Lu, F.; Chen, J.; Lu, R.; Huang, Q.; Jiang, H.; Taarning, E.; Xu, J., A strategy for generating high-quality cellulose and lignin simultaneously from woody biomass. *Green Chemistry* **2017,** *19* (20), 4849-4857.
48. Román-Leshkov, Y.; Chheda, J. N.; Dumesic, J. A., Phase modifiers promote efficient production of hydroxymethylfurfural from fructose. *Science* **2006,** *312* (5782), 1933-1937.
49. Athaley, A.; Annam, P.; Saha, B.; Ierapetritou, M., Techno-economic and life cycle analysis of different types of hydrolysis process for the production of p-Xylene. *Computers & Chemical Engineering* **2019,** *121*, 685-695.
50. Athaley, A.; Saha, B.; Ierapetritou, M., Biomass-based chemical production using techno-economic and life cycle analysis. *AIChE Journal* **2019,** *65* (9), e16660.
51. Wooley, R. J.; Putsche, V. *Development of an ASPEN PLUS physical property database for biofuels components*; National Renewable Energy Lab., Golden, CO (United States): 1996.
52. Hirshleifer, J., On the theory of optimal investment decision. *Journal of political economy* **1958,** *66* (4), 329-352.

53. Modenbach, A. A.; Nokes, S. E., The use of high-solids loadings in biomass pretreatment—a review. *Biotechnology and Bioengineering* **2012,** *109* (6), 1430-1442.
54. Humbird, D.; Davis, R.; Tao, L.; Kinchin, C.; Hsu, D.; Aden, A.; Schoen, P.; Lukas, J.; Olthof, B.; Worley, M. *Process design and economics for biochemical conversion of lignocellulosic biomass to ethanol: dilute-acid pretreatment and enzymatic hydrolysis of corn stover*; National Renewable Energy Lab.(NREL), Golden, CO (United States): 2011.
55. Abbati de Assis, C.; Greca, L. G.; Ago, M.; Balakshin, M. Y.; Jameel, H.; Gonzalez, R.; Rojas, O. J., Techno-economic assessment, scalability, and applications of aerosol lignin micro- and nanoparticles. *ACS sustainable chemistry & engineering* **2018,** *6* (9), 11853-11868.